

A QUASI-PARAPOTENTIAL MODEL
FOR THE HIGH v/γ DIODE

by John Creedon

PIIR-19-70

May 1970

Prepared by
Physics International Company
2700 Merced Street
San Leandro, California 94577

DEFINITION OF SYMBOLS

I_0	= anode current (amps)
V_0	= anode potential (volts)
R_c	= cathode radius (m)
d	= anode-cathode spacing (m)
β_0	= u_0/c
u_0	= velocity of the electrons at the anode (m/sec)
c	= velocity of light (m/sec)
γ_0	= $1/(1 - \beta_0^2)^{1/2}$
m_0	= rest mass of the electron (kg)
e	= charge of the electron (coulombs)
I_1	= limiting current for Child's Law (amps)
B_ϕ	= azimuthal component of magnetic flux density (webers/m ²)
μ_0	= permeability of free space = $4\pi \times 10^{-7}$ (henry/m)
R	= radial distance measured from the axis of the diode (m)
j	= current density (amps/m ²)
\vec{E}	= electric field strength (volts/m)
\vec{u}	= velocity of the electrons at any point in the diode (m/sec)
\vec{B}	= magnetic flux density (webers/m ²)
V	= potential at any point in the diode (volts)
r	= distance from origin of the spherical polar coordinate system (m)
θ, ϕ	= polar and azimuthal angles of the spherical polar coordinate system (radians)
$\vec{e}_r, \vec{e}_\theta, \vec{e}_\phi$	= unit vectors in the spherical polar coordinate system

- δ = polar angle of equipotential for which $V = 0$ (radians)
- ρ = charge density (coulombs/m³)
- ϵ_0 = permittivity of free space = $10^{-9}/36\pi$ (farad/m)
- I = total current inside an equipotential (amps)
- β = u/c
- γ = $1/(1 - \beta^2)^{1/2}$
- $g(\theta)$ = angular charge density (coulombs/m)
- k = integration constant for solution of Equation (16)

SUMMARY

A model for the high v/γ diode is proposed in which the electron flow is parapotential (i.e., along the equipotentials) except for a small region around the axis. On the basis of this model, the anode current of the diode is expressed as a function of the anode potential and the ratio of the cathode radius to the anode-cathode spacing.

CONTENTS

	<u>Page</u>
I INTRODUCTION	1
II A QUASI-PARAPOTENTIAL MODEL	6
III RELATIONSHIP BETWEEN CURRENT AND POTENTIAL FOR CONICAL EQUIPOTENTIALS	12
References	21

ILLUSTRATIONS

<u>Figure</u>		<u>Page</u>
1	Diode Configuration	2
2	Comparison of Child's Law and Critical Current	4
3	Schematic of Electron Flow	8
4	Coordinate System for Diode Calculations	10
5	Results of Numerical Calculations	16
6	Current Versus Potential for Child's Law and Parapotential Flow	17
7	Current Versus Potential for Parapotential Flow	18

SECTION I
INTRODUCTION

The diodes considered in this report have the form shown in Figure 1. The anode is a plane, the cathode shank is a cylinder of radius R_c , and the flat face of the cathode is spaced a distance d from the anode. The current is presumed to have only radial and axial components and it is assumed to be cylindrically symmetrical. Only the steady-state case is considered.

The actual cathodes used consist of a large number of needles or some other kind of roughened surface so that the emission process is almost certainly initiated by field emission. However, there is evidence that a plasma forms at the cathode and provides a copious supply of electrons (Reference 1). It has been shown (References 2, 3, and 4) that a macroscopic field of about 10^5 V/cm at the surface of a metal will be enhanced by microscopic protrusions on the surface, and that the field emission currents generated in these protrusions are capable of vaporizing the protrusions. The existence of this plasma at the cathode is the basis for the treatment of these diodes as "space charge limited," that is, the cathode current increases until the space charge of the electrons depresses the electric field to zero at the cathode.

For the space-charge-limited case and a sufficiently low potential difference between the cathode and anode, one can apply nonrelativistic Child's law theory, (Reference 5) for plane-parallel electron flow. The expression for anode current is (neglecting fringing effects, etc.)

$$I_o = 2.335 \times 10^{-6} \pi \left[\frac{R_c}{d} \right]^2 V_o^{3/2} \quad (1)$$

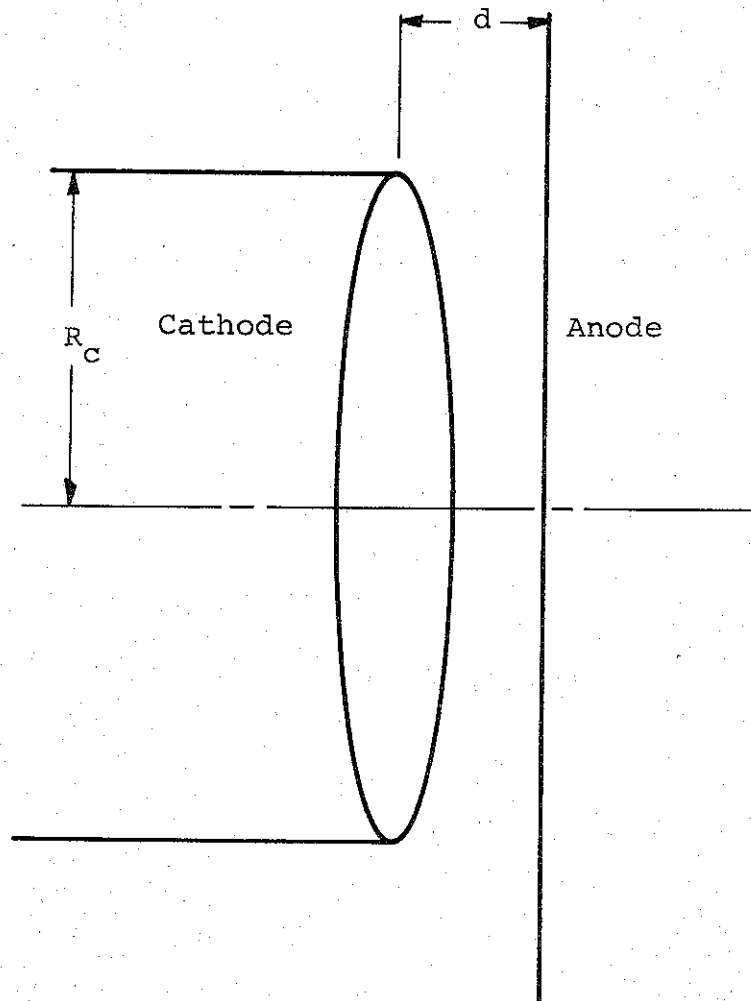


FIGURE 1. DIODE CONFIGURATION

All symbols used in this report are defined (Page iv).

As the potential of the anode is increased one must modify Equation (1) for two reasons:

1. For plane-parallel flow the relation between the velocity and the kinetic energy of the electrons must be modified for relativistic effects.
2. The self-magnetic field of the electrons causes the electron trajectories to be curved toward the axis.

The relativistic velocity correction has been carried out by several authors (References 1, 6, and 7) and is essentially negligible for an anode potential below 500 kV.

The self-magnetic field effects become important at considerably lower potentials. An upper limit for the diode current for which one may neglect self-magnetic field effects is given by (References 1 and 6)

$$I_1 = 8500 \beta_o \gamma_o (R_c/d) = 8500 \left[(eV_o/m_o c^2)^2 + 2 (eV_o/m_o c^2) \right]^{1/2} (R_c/d) \quad (2)$$

Figure 2 is a plot of the currents from Equation (1) and (2) versus anode potential. For $R_c/d = 10$ the self-magnetic field limit occurs at 260 kV.

Equation (2) is a rough approximation derived by equating the radius of curvature of an electron traveling in the magnetic field at the edge of the beam (with energy corresponding to the anode potential), to the spacing d .

Child's Law Current: $I_0 = 2.335 \times 10^{-6} \pi \left(\frac{R_c}{d}\right)^2 V^{3/2}$

Critical Current: $I_1 = 8500 \beta_o \gamma_o \frac{R_c}{d}$

$\frac{R_c}{d} = 10.0$

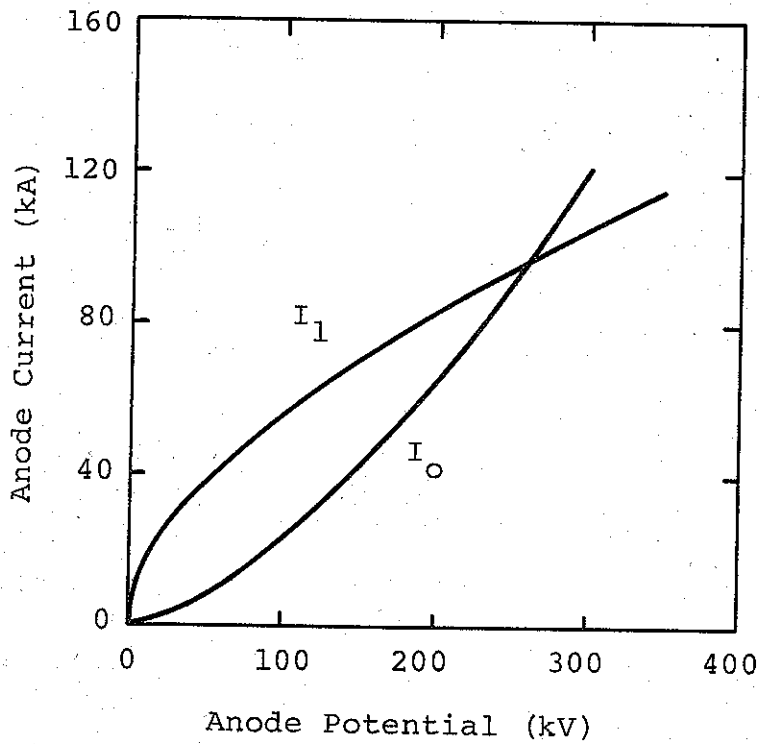


FIGURE 2. COMPARISON OF CHILD'S LAW AND CRITICAL CURRENT

The actual limiting value of current for the validity of Child's law is smaller than that calculated from Equation (2), but difficult to express analytically.

Numerical schemes have been developed (References 1 and 6) to calculate electron trajectories in a consistent manner, but the computer codes exhibit convergence problems when the self-magnetic forces begin to dominate the problem.

The problem of the very-high-current diode in many ways suggests the Brillouin type of electron flow that exists in crossed field microwave tubes (Reference 8). The electron flow in these devices is perpendicular to both the electric and magnetic fields.

dePackh (References 9 and 10) explored just such a possibility when he calculated the parapotential (i.e., along equipotentials) flow in a diode with conical cathode and anode.

The remainder of this report is devoted to the development of a parapotential flow model for the diode in Figure 1.

SECTION II

A QUASI-PARAPOTENTIAL MODEL

The object of any model for electron flow in a diode is a consistent solution for the coupled equations that describe the interaction of the electromagnetic fields and the motion of the electrons. In other words, the motion of the electrons under the influence of the electromagnetic fields will give a certain space charge distribution. This distribution, when combined with the equations of the electromagnetic fields and the boundary conditions, must give the original fields.

The model proposed in this report is not completely consistent in the above sense. The principal assumption of the model is that the electron flow is parapotential in most of the diode, but that there is a small region around the axis in which the electrons travel across the equipotentials to reach the anode. The total current carried by the electrons is calculated as a function of the anode potential by neglecting this small region around the axis.

The reason that the electrons make the transition from parapotential flow to flow across the equipotential near the axis is intuitively obvious. When an electron traveling on an equipotential enters the region where the electrons are flowing across the equipotential, the magnetic field starts to decrease. There is no longer a balance between \vec{E} and $\vec{u} \times \vec{B}$ and the electron pulls away from the equipotential toward the anode. When an electron crosses the axis the force due to the magnetic field reverses and both the \vec{E} and $\vec{u} \times \vec{B}$ forces are in the general direction of the anode.

Other features of the model may be seen by referring to Figure 3. The emission is assumed to occur principally at the edges of the cathode and on the cathode shank. The emission for most of the central area of the cathode is suppressed because the electron sheath has depressed the potential to zero in this region. The details of how the electrons leave the cathode edge or shank and reach higher equipotentials are not considered.

It is at least plausible that the anode current is limited by the amount of current that can flow from the edge of the cathode to the axis, and that one can calculate this current without considering in detail the process that occurs at the axis. Even if the model were completely consistent, it would not necessarily guarantee the uniqueness of a solution of the coupled equations. The justification for any model of the diode must depend on experimental verification.

Because of the symmetry and the lack of an azimuthal component of current, the magnetic field in the diode has only an azimuthal component. The magnetic field is given by

$$B_{\phi} = (\mu_0/2\pi R) \int \vec{j} \cdot \vec{d}\sigma$$

where R is the radial distance from the axis and $\int \vec{j} \cdot \vec{d}\sigma$ is taken over an area whose boundary is the circle (centered on the axis) of radius R located in a plane parallel to the anode.

For the steady state, the equation of continuity gives

$$\nabla \cdot \vec{j} = 0$$

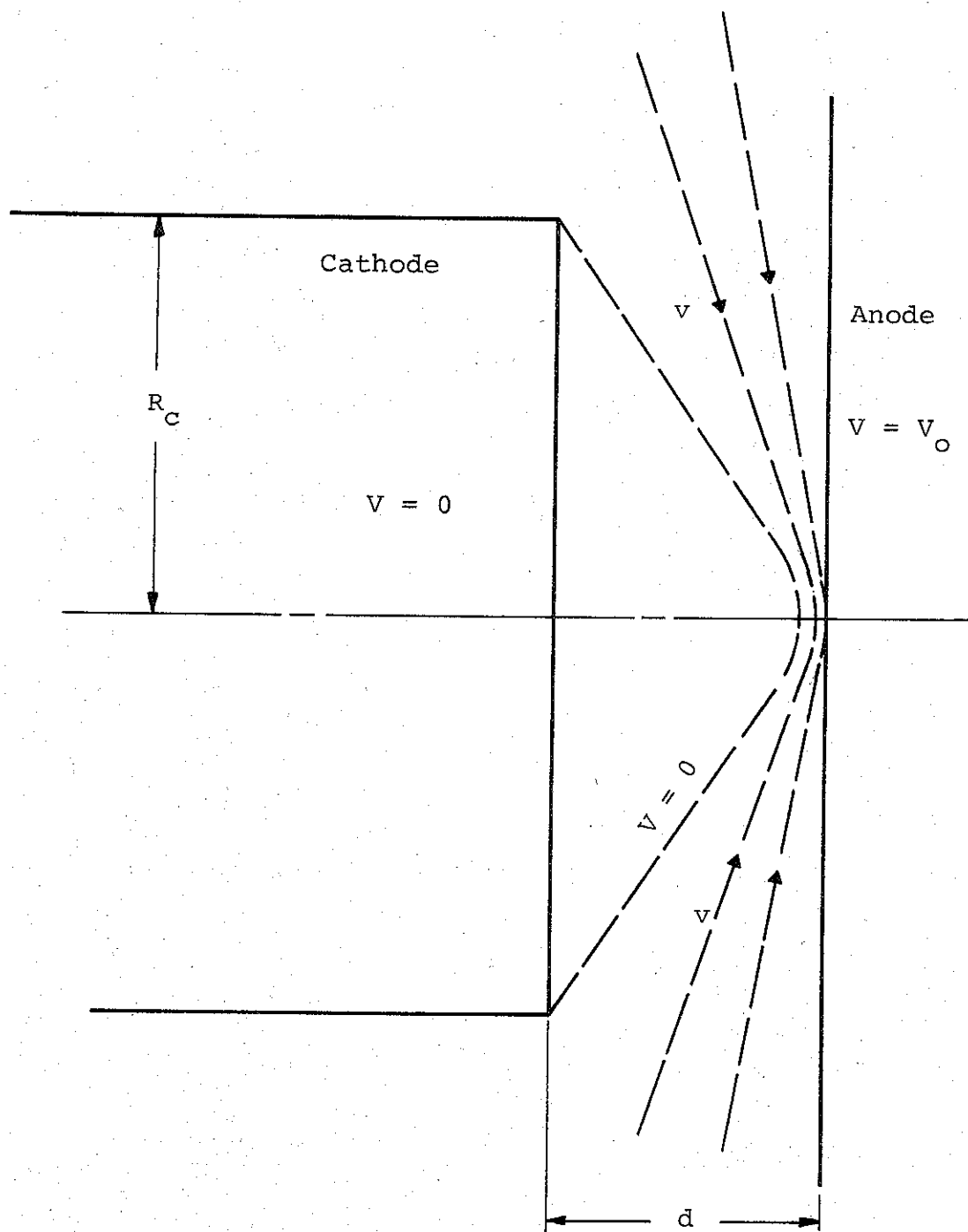


FIGURE 3. SCHEMATIC OF ELECTRON FLOW

From the divergence theorem and the assumption of electron flow along equipotentials one can see that

$$\int \vec{j} \cdot \vec{d\sigma}$$

(taken over an area as specified above) is a constant for any point on a given equipotential. Therefore along an equipotential

$$B_{\phi} \propto \frac{1}{R}$$

The parapotential flow condition for an equipotential that is approximately straight is

$$\vec{E} = - \vec{u} \times \vec{B}$$

and since u is a constant

$$E = |\nabla V| \propto \frac{1}{R} \quad (3)$$

along any equipotential.

Now consider a polar coordinate system with its z axis along the axis of the diode and with its origin at the anode surface (see Figure 4). The form for the gradient in spherical polar coordinates

$$\nabla V = \frac{\partial V}{\partial r} \vec{e}_r + \frac{1}{r} \frac{\partial V}{\partial \theta} \vec{e}_{\theta} + \frac{1}{r \sin \theta} \frac{\partial V}{\partial \phi} \vec{e}_{\phi}$$

suggests a very simple set of equipotentials. If V is only a function of the polar angle θ then

$$V = V(\theta)$$

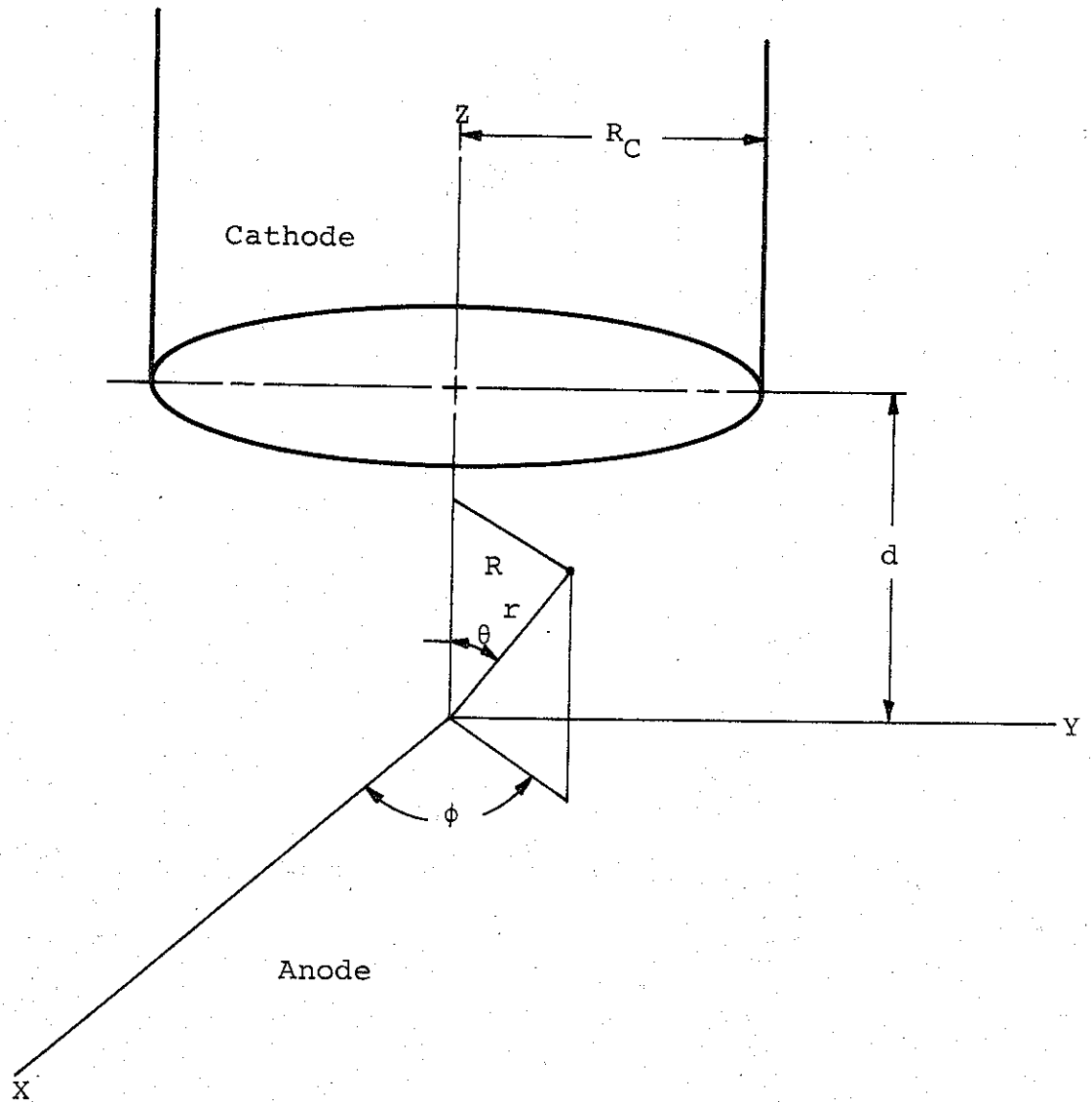


FIGURE 4. COORDINATE SYSTEM FOR DIODE CALCULATIONS

and

$$E = \frac{1}{r} \frac{\partial V}{\partial \theta}$$

The equipotentials are the cones

$$\theta = \text{constant}$$

and the condition in Equation (3) is satisfied since

$$R = r \sin \theta$$

These considerations result in what is perhaps the simplest possible set of equipotentials. Of course, there is no guarantee of uniqueness.

There is one final assumption made in this model. It seemed only natural to associate the angle δ of the equipotential for which $V = 0$, with the angle subtended by the edge of the cathode (see Figure 1)

$$\delta = \tan^{-1} (R_c/d)$$

SECTION III

RELATIONSHIP BETWEEN CURRENT AND POTENTIAL
FOR CONICAL EQUIPOTENTIALS

The system of equations that must be solved is (see Definition of Symbols)

Poisson's equation

$$\nabla^2 v = - \frac{\rho}{\epsilon_0} \quad (4)$$

Current inside a given equipotential

$$I = \int \rho \vec{u} \cdot d\vec{\sigma} \quad (5)$$

Parapotential flow condition

$$\vec{E} = - \vec{u} \times \vec{B} \quad (6)$$

Magnetic field

$$B_\phi = \frac{\mu_0 I}{2\pi R} \quad (7)$$

Relationship between electron velocity and potential

$$u = \beta c = c \left[1 - \frac{1}{\gamma^2} \right]^{\frac{1}{2}} \quad (8)$$

$$\gamma = \frac{eV + m_0 c^2}{m_0 c^2}$$

From the divergence theorem and the conical flow lines for j one can see that

$$j \propto \frac{1}{r^2}$$

on an equipotential, and since the velocity u is a constant, the charge density must have the form

$$\rho = g(\theta)/r^2$$

where $g(\theta)$ is some function to be determined. With this expression for charge density Equations (4) through (7) can be written in spherical polar coordinates as

$$\frac{d^2V}{d\theta^2} + \frac{\cos \theta}{\sin \theta} \frac{dV}{d\theta} = - \frac{g(\theta)}{\epsilon_0} \quad (9)$$

$$I(\theta) = - 2\pi \int_{\delta}^{\theta} g(\theta') \beta(\theta') c \sin \theta' d\theta' \quad (10)$$

$$\frac{dV}{d\theta} = \frac{\beta c \mu_0 I}{2\pi \sin \theta} \quad (11)$$

where

$$V(\delta) = 0$$

If one differentiates Equations (10) and (11), eliminates $dI/d\theta$, combines this expression with Equation (8), and substitutes the resulting expression for $g(\theta)$ in Equation (9) one gets, after some manipulation

$$\frac{d^2 \gamma}{d\theta^2} + \frac{\cos \theta}{\sin \theta} \frac{d\gamma}{d\theta} = \frac{\gamma}{\gamma^2 - 1} \left(\frac{d\gamma}{d\theta} \right)^2 \quad (12)$$

the boundary conditions are

$$\begin{aligned} \gamma(\delta) &= 1 \\ \gamma(\pi/2) &= \frac{eV_o + m_o c^2}{m_o c^2} \end{aligned}$$

where V_o = anode potential and δ is the angle of the equipotential for which $V = 0$

The current flowing between angles δ and θ is given by [from Equations (11) and (8)]

$$I(\theta) = (2\pi/\mu_o c) (m_o c^2/e) (\sin \theta/\beta) \frac{d\gamma}{d\theta} = 8500 \frac{\sin \theta}{\beta} \frac{d\gamma}{d\theta} \quad (13)$$

and the anode current is

$$I_o = \frac{8500}{\beta_o} \frac{d\gamma}{d\theta}$$

$$\text{for } \theta = \frac{\pi}{2}$$

If one specifies both the anode potential and the anode current, then both γ and $d\gamma/d\theta$ have been fixed for $\theta = \pi/2$. An application of the standard uniqueness theorem for differential equations (Reference 11) ensures a unique solution for Equation (12) as long as $\gamma > 1$ and $0 < \theta \leq \pi/2$. However, for $\gamma = 1$, neither the continuity condition or the Lipschitz condition are satisfied, and, in fact, there is a whole family of solutions for which

$$\gamma(\delta) = 1, \quad \left. \frac{d\gamma}{d\theta} \right|_{\delta} = 0$$

for any angle δ .^{*} This multiplicity of solutions creates no difficulty since each member of the family corresponds to a different value of anode current and potential.

Because of the nonlinearity of Equation (12) a numerical solution was used to find γ as a function of θ . The procedure consisted of specifying the potential and current at the anode (and thus γ and $d\gamma/d\theta$) and solving for δ . Figure 5 contains the results of these calculations as a plot of anode current versus R_c/d (i.e., $\tan \delta$) for various anode potentials.

From the data in Figure 5, one can plot curves of anode current versus anode potential for constant values of R_c/d . These relationships are presented in Figures 6 and 7.

The dotted curve in Figures 6 and 7 is the boundary between the region where Child's law is valid and the region where the effect of the self-magnetic field becomes dominant. The expression for the boundary curve comes from equating I_0 and I_1 in Equations (1) and (2) and eliminating R_c/d .

$$I_0 = 38.0 \frac{V_0 + 2 (m_0 c^2/e)}{V_0^{1/2}} \quad (15)$$

* From Equations (10) and (11) it can be seen that $d\gamma/d\theta$ must be zero for $\gamma = 1$ since $I = 0$ for $\theta = \delta$.

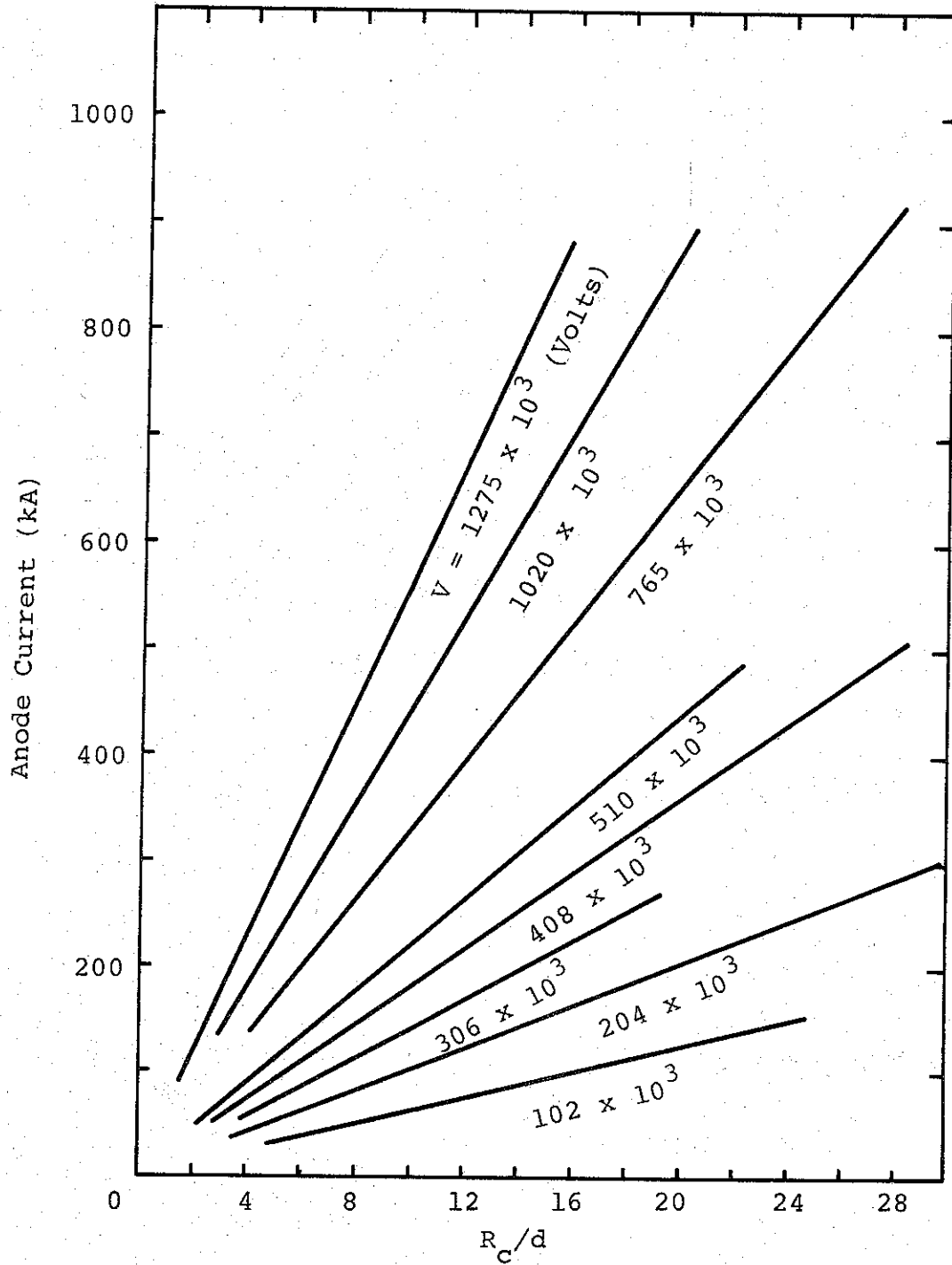


FIGURE 5. RESULTS OF NUMERICAL CALCULATIONS

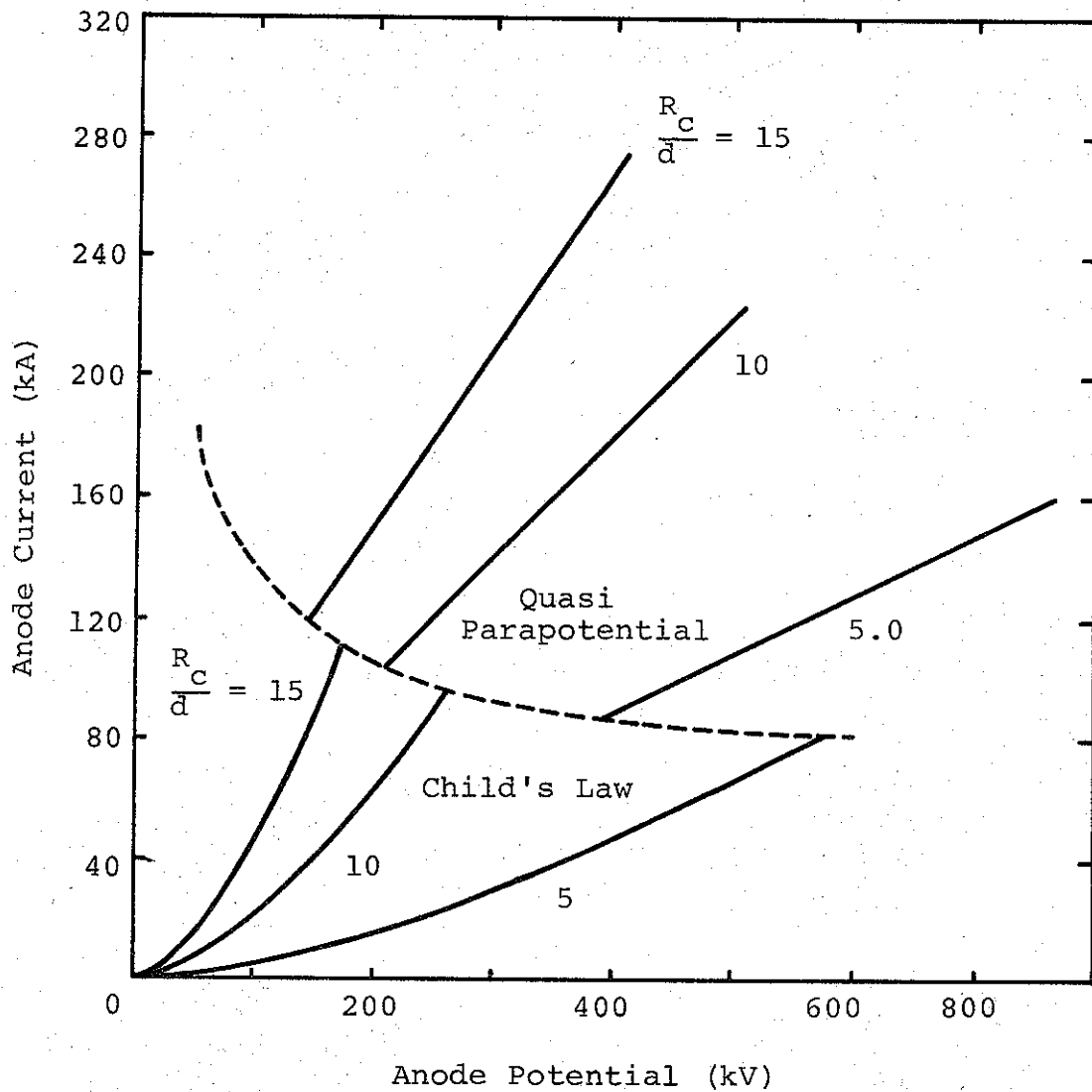
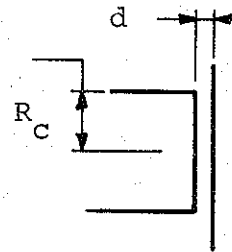


FIGURE 6. CURRENT VERSUS POTENTIAL FOR CHILD'S LAW AND PARAPOTENTIAL FLOW

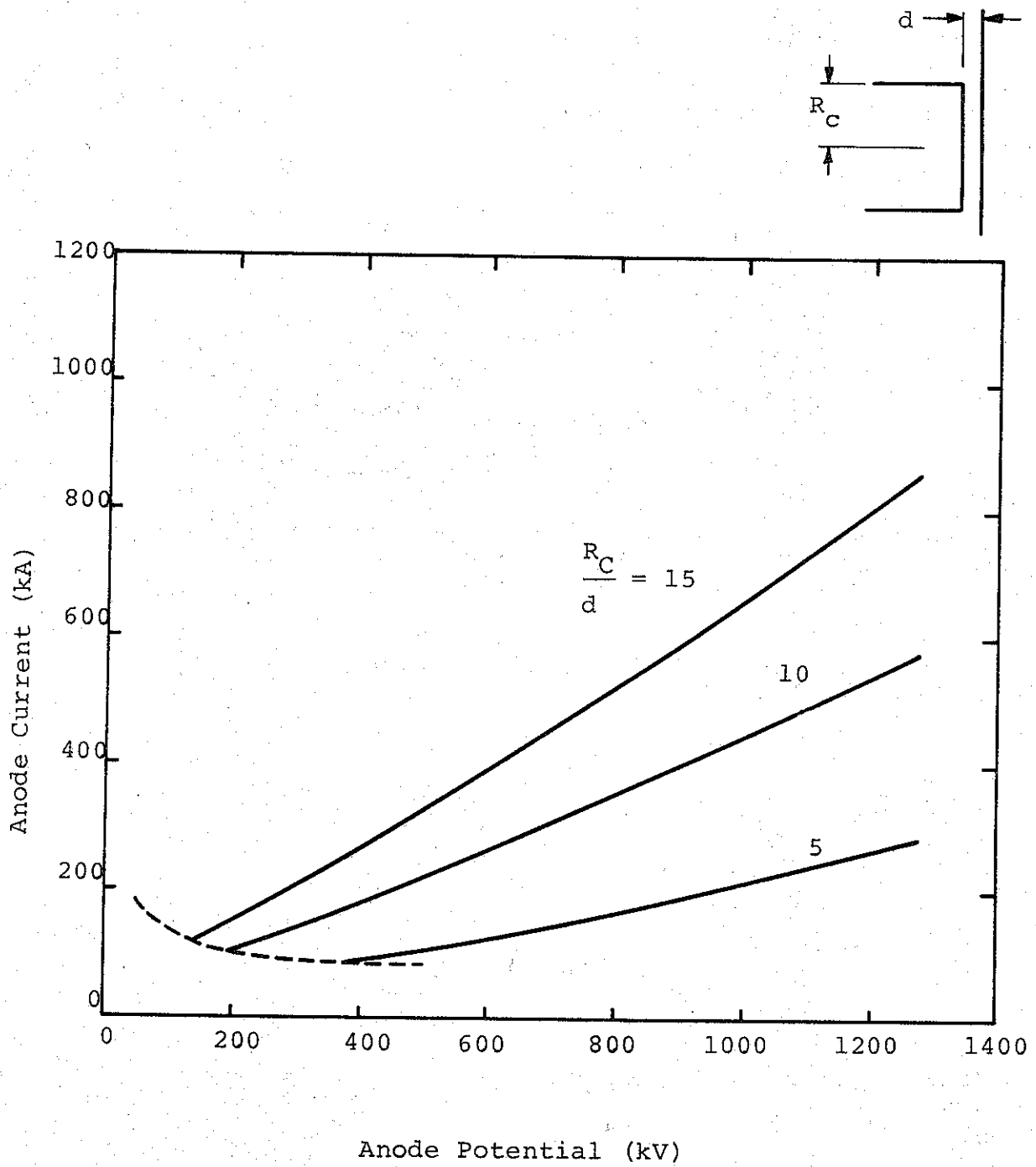


FIGURE 7. CURRENT VERSUS POTENTIAL FOR PARAPOTENTIAL FLOW

This boundary occurs in a region for which neither Child's law nor the parapotential flow relations can be correct. It would be necessary to develop some kind of solution in the transition region to connect the Child's law curves with the parapotential curves.

It is possible to obtain an approximate analytical solution to Equation (12) by neglecting the second term on the left-hand side. The justification for this is obvious when $d\gamma/d\theta \gg 1$ and $\tan \theta > 1$, however the results of the numerical solution indicate that the approximation is valid (for $\tan \theta > 1$) as $d\gamma/d\theta \rightarrow 0$ because $\gamma^2 - 1 \rightarrow 0$.

The approximate differential equation is

$$\frac{d^2\gamma}{d\theta^2} = \frac{\gamma}{\gamma^2 - 1} \left(\frac{d\gamma}{d\theta} \right)^2 \quad (16)$$

and the solution is

$$\theta = k \ln [\gamma + (\gamma^2 - 1)^{1/2}] + \delta \quad (17)$$

differentiating Equation (17) once gives

$$\frac{d\gamma}{d\theta} = \frac{1}{k} (\gamma^2 - 1)^{1/2} \quad (18)$$

This solution has all the properties of the exact solution. k and δ are the constants of integration, also

$$\gamma = 1 \text{ implies that } \theta = \delta$$

and for any δ

$$\gamma = 1 \text{ implies that } \frac{d\gamma}{d\theta} = 0$$

The specification of $\gamma = 1$ and $d\gamma/d\theta = 0$ at δ does not determine a unique solution.

The boundary conditions can be applied to determine k . From Equation (17) for $\theta = \pi/2$

$$k = \frac{\pi/2 - \delta}{\ln [\gamma_0 + (\gamma_0^2 - 1)^{1/2}]} \quad (19)$$

Combining Equations (8), (13), and (18) gives

$$I = \frac{8500 \gamma \sin \theta}{k}$$

substituting for k from Equation (19) and setting $\theta = \pi/2$ gives

$$I_0 = \frac{8500 \gamma_0 \ln [\gamma_0 + (\gamma_0^2 - 1)^{1/2}]}{\pi/2 - \tan^{-1} (R_c/d)} \quad (20)$$

where as before $\delta = \tan^{-1} (R_c/d)$

There is good agreement between values calculated from Equation (20) and the numerical solutions plotted in Figures 6 and 7. It is interesting to note that by expanding $\tan^{-1} x$

$$\tan^{-1} x = \frac{\pi}{2} - \frac{1}{x} + \frac{1}{3x^3} - \frac{1}{5x^5} + \dots \quad \text{for } x^2 > 1$$

(see Reference 12) Equation (20) becomes

$$I_0 \approx 8500 \frac{R_c}{d} \gamma_0 \ln \left[\gamma_0 + (\gamma_0^2 - 1)^{1/2} \right] \quad (21)$$

This expression is consistent with the straight line variation of I with R_c/d plotted in Figure 5 from the numerical solution.

REFERENCES

1. "Research on Beam Stopping Due To Self-Magnetic Compression," DASA 2167, Ion Physics Corporation (Nov. 1968).
2. F. Charbonnier, C. Bennett, and L. Swanson, "Electrical Breakdown between Metal Electrodes in High Vacuum," J. Appl. Phys. Vol. 38, No. 2, 627-640 (Feb. 1967).
3. R. Little, W. Whitney, "Electron Emission Preceding Electrical Breakdown in Vacuum," J. Appl. Phys. Vol. 34, No. 8, 2430-2432 (Aug. 1963).
4. W. Dyke, J. Trolan, E. Martin, and J. Barbour, "The Field Emission Initiated Vacuum Arc," Phys. Rev. Vol. 91, No. 5, 1043-1057 (Sept. 1953).
5. K. Spangenberg, Vacuum Tubes, (McGraw-Hill, New York, 1948).
6. F. Friedlander, R. Hechtel, H. Jory, and C. Mosher, "Megavolt-Megampere Electron Gun Study," DASA 2173, Varian Associates (Sept. 1968).
7. W. Howes, "One-Dimensional Space-Charge Theory. II. Relativistic Child's Law," J. Appl. Phys., Vol. 37, No. 1, pp. 438-439 (Jan. 1966).
8. Crossed-Field Microwave Devices, edited by E. Okress, (Academic Press, New York, 1961).
9. D. C. dePackh, "Parapotential Flow," Project Progress Report No. 5, Naval Research Laboratory, Washington, D. C. (Dec. 1969).
10. D. C. dePackh, "Parapotential Electron Flow and the Vacuum Pinch," Radiation Project Internal Report No. 7, Naval Research Laboratory, Washington, D. C., (April 1968).
11. L. R. Ford, Differential Equations (McGraw-Hill, New York 1933).
12. H. B. Dwight, Tables of Integrals and Other Mathematical Data (MacMillan and Co., New York 1949).